Prediction of Roll Moments on Finned Bodies in Supersonic Flow

WILLIAM L. OBERKAMPF*
The University of Texas at Austin, Austin, Texas

A method is presented for predicting roll moments produced by fins on missile bodies at high angle of attack in supersonic flow. The missile configurations are assumed to have pointed noses and circular cylindrical bodies. The effect of the body induced flow on the roll moments produced by fins is studied. Particular attention is given to the body vortices and separated flow on the lee side of the missile. A cruciform fin configuration with fins having rectangular planform is analyzed. A previously developed flow model is used to calculate the flowfield produced by the body. The body flowfield experienced by the fins is used with a quasi-linear lifting theory to predict the roll moments. Results are presented for the fin cant, induced roll, and roll damping moments. The roll moment predictions are compared with experimental data and generally good agreement is obtained. The physical causes of the observed nonlinear roll phenomena are discussed.

Nomenclature

a = body radius
b_0 = fin semi-span
c = fin chord
C_l = roll moment coefficient ($l/q\,S_b\,d$)
C_{l_p} = roll damping moment coefficient derivative ($\partial C_l/\partial p$)
C_{l_δ} = fin cant moment coefficient derivative $(\partial C_l/\partial\delta)_{\delta\to 0}$
d = body diameter
l = roll moment
M = Mach number of freestream
N = normal force
N_v = total number of vortices in flow model
p = dimensionless rolling speed, ($\dot{\phi} b_0/U_\infty$)
p_b, p_t = local pressure on bottom and top surface of fin, respectively
$\hat{p}_b, \hat{p}_t$ = local pressure coefficient on bottom and top surface of fin, respectively
q = dynamic pressure of freestream
r_c = radius of vortex core
r_{3D} = radial coordinate of tip Mach cone
S_b = frontal area of the missile body (πa^2)
t_f = thickness of the fin
u, v, w = velocities in the x, y, z directions, respectively (Fig. 1)
U_∞ = freestream speed
U_c = cross-flow freestream speed, $U_\infty \sin\alpha_b$
$\mathbf{V}$ = velocity ($u\mathbf{i}+v\mathbf{j}+w\mathbf{k}$)
x_l, x_t = x coordinate of fin leading and trailing edge, respectively
x_s = x coordinate of boundary-layer separation point
x, y, z = coordinate system (Fig. 1)
α_b = angle of attack of the body
α_l = local angle of attack of fin
β = $(M^2-1)^{1/2}$
γ = ratio of specific heats of freestream
θ_b, θ_t = local flow turn angle on bottom and top surface of fin, respectively
θ_f = half-angle of fin wedge
δ = fin cant angle
ϕ = roll angle measured from y axis
$\dot{\phi}$ = roll rate

Subscripts
c = cross-flow
$2D$ = two-dimensional flow
$3D$ = three-dimensional flow

Presented as Paper 74-111 at the AIAA 12th Aerospace Sciences Meeting, Washington, D.C., January 30–February 1, 1974; submitted March 4, 1974; revision received August 30, 1974.

Index categories: LV/M Aerodynamics; LV/M Dynamics and Control; Supersonic and Hypersonic Flow.

* Assistant Professor, Department of Mechanical Engineering. Associate Member AIAA.

Introduction

THE importance of roll moments on the flight dynamic characteristics of finned bodies is well recognized. As missiles are required to operate at higher angles of attack, nonlinear roll moment phenomena need to be more clearly understood and accurately predicted. The theoretical prediction of roll moments produced by finned bodies at high angle of attack in supersonic flow has been relatively unsuccessful up to the present time. As a result, the missile designer has been ineffective in this area and the roll moment characteristics of missile configurations have been determined by extensive wind tunnel testing. This has proven to be a time-consuming and costly task for new or modified configurations.

The flowfield of a circular cylindrical body at high angle of attack is dominated by the presence of body vortices and separated flow on the lee side. These vortices increase in strength as the angle-of-attack or body length increases. A theoretical model for the body flowfield has been previously developed by Mello and Sivier.[1,2] This model was later extended and improved in Refs. 3 and 4. Mello and Sivier, using their flow model and three different lifting theories, attempted to predict the induced roll moment of a finned body. Although their method did not prove to be generally successful, they did point out several of the important parameters affecting the induced roll moment.

The approach taken by Mello and Sivier, and also the present approach, assumes that the body vortices are not affected by the fin induced flowfield. This implies that the present approach is not appropriate for very low aspect ratio fins. For the very low aspect ratio case, the body vortex paths are substantially affected by the presence of the fins as they travel down the body. The slender body approach, similar to that developed by Spahr,[5] is the most appropriate for very low aspect ratio fins.

In the present paper a method for predicting roll moments produced by finned bodies at high angle of attack in supersonic flow is presented. A cruciform fin configuration with fins having rectangular planform is analyzed; however, a three fin configuration can be studied by a simple modification of the present method. The model of the body flowfield presented in Refs. 3 and 4 is used in the present investigation. Included in this flow model are the concentrated body vortices, vortex sheets, and core regions of the concentrated body vortices. The flow model is used in conjunction with a here-in developed quasi-linear lifting theory to predict roll moments. The lifting theory is a combination of a series expansion method and linear conical flow theory. The roll moment predictions of the present method are compared with experimental data.

Aerodynamic Analysis

The foundation of the present aerodynamic analysis is the assumption that the body flowfield is not affected by the flowfield induced by the fin. That is, it is assumed that the flowfield generated by the body affects the flowfield experienced by the fins but that the fin induced flow does not, in turn, alter the body flowfield. Following from this assumption the aerodynamic analysis of roll moments produced by the fins can be divided into two parts: first, the flowfield generated by the body, and second, the lifting theory and roll moment prediction for the fins. The model of the body flowfield will be discussed only briefly because this has been given previously in Refs. 3 and 4. The lifting theory will then be presented in some detail.

Body Flowfield

The dominant flowfield characteristic of a body of revolution at high angle of attack is the presence of body vortices which form on the lee side (Fig. 1). The strength of these vortices increases both with angle of attack and length down the body. To model this complex separated flowfield it is assumed that the flow can be divided into cross flow and axial flow. For the present case of supersonic freestream flow, it is also assumed that the cross-flow can be considered as incompressible. This is a good assumption as long as $M \sin\alpha_b < 1$. The three-dimensional body flowfield is formed by vectorially adding the flow velocities in the cross-flow plane to the axial component of velocity so that

$$\mathbf{V} = U_\infty \cos\alpha_b \mathbf{i} + v_c \mathbf{j} + w_c \mathbf{k}$$

where v_c and w_c are given in Ref. 3.

The body vortices are regions of concentrated vorticity on the lee side of the body. Outside of the core region these vortices are modeled by potential flow vortices. In the core region an exponential decay of the vortex tangential velocity is used to model the physical flow. Vortex sheets feed vorticity from the boundary layer on the body into the concentrated body vortices. The vortex sheets are modeled by a large number (40) of low strength potential flow vortices in the cross-flow plane (Fig. 2). It can be seen from Fig. 2 that the vortex sheets will strongly increase the tendency of flow separation on the lee side of the body.

The strength and position of the body vortices, and the relative strength of the vortex sheets are taken from experimental data of Mello[2] for $M = 2$. The interpolation of the experimental data for various angles of attack and body lengths is given in Ref. 4. The radius of the vortex core r_c is taken to be

$$r_c/a = 0.06\alpha_b{}^{1/2} x/a$$

This equation is based on the experimental data of Mello[2] and Jorgensen and Perkins.[6] Although there is considerable scatter in the data with respect to angle of attack, this equation correlates the data fairly well.

Lifting Theory

Consider a fin with straight leading and trailing edges perpendicular to the axis of the missile and the tip chord parallel to the axis of the missile. The differential normal force dN on a differential element dx by dr is written as

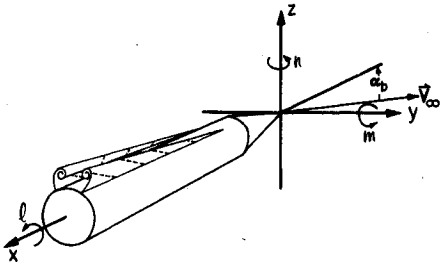

Fig. 1 Body vortex wake and coordinate system.

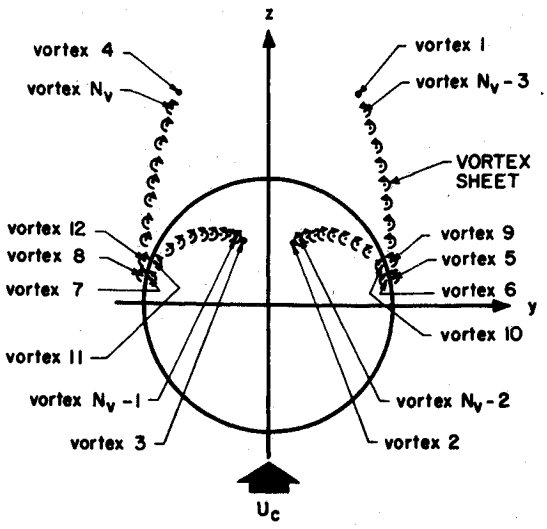

Fig. 2 Cross-flow plane of flow model (from Ref. 3).

$$dN = (p_b - p_t)\, dr\, dx$$

This equation can be written in terms of the pressure coefficient $\hat{p}$ as

$$dN = (\hat{p}_b - \hat{p}_t) q\, dr\, dx \tag{1}$$

With this arrangement it is assumed that the flow properties after the shock wave generated by the nose are approximately the same as the freestream conditions.

Now consider the pressure field generated by the fin. The flow about a fin can be divided into a two-dimensional (2-D) and a three-dimensional (3-D) region. The division line between the regions is the Mach cone emanating from the leading edge of the fin tip. The calculation of pressure on the upper and lower surfaces of the fin in the 2-D region could be calculated by shock-expansion theory. This theory is rather cumbersome and the accuracy afforded is not necessary in light of the previously made simplifying assumptions. Instead, the surface pressure is calculated in the 2-D region by means of a three term series expansion in terms of flow turn angle θ. These equations given in terms of the pressure coefficient $\hat{p}$ are[7]

$$\hat{p} = C_1\theta + C_2\theta^2 + C_3\theta^3 \qquad \theta < 0 \tag{2a}$$

$$\hat{p} = C_1\theta + C_2\theta^2 + (C_3 - D)\theta^3 \qquad \theta > 0 \tag{2b}$$

where

$$C_1 = 2/\beta$$

$$C_2 = [(M^2-2)^2 + \gamma M^4]/(2\beta^4)$$

$$C_3 = \frac{M^4}{\beta^7}\left[\frac{\gamma+1}{6}\left(M^2 - \frac{5+7\gamma-2\gamma^2}{2(\gamma+1)}\right)^2 + \frac{-4\gamma^4+28\gamma^3+11\gamma^2-8\gamma-3}{24(\gamma+1)}\right] + \frac{3(M^2-\frac{4}{3})^2}{4\beta^7}$$

$$D = (\gamma+1)M^4[(5-3\gamma)M^4 - (12-4\gamma)M^2 + 8]/(48\beta^7)$$

Equation (2a) is used for expansive flow and Eq. (2b) for compressive flow. The three-term series expansion enables one to calculate simply and accurately the pressure coefficient for large angles of attack.

The pressure coefficient in the 3-D region is calculated by a combination of conical flow theory and the previously given series expansion method. Conical flow theory is used to determine the functional variation of the pressure coefficient over the 3-D region. The level, or magnitude, of the function is determined by matching it to the pressure coefficient in the 2-D region along the tip Mach cone. In this way the value of the pressure coefficient in the 3-D region will be somewhat more accurate than linear theory alone because of matching to the series expansion method.

Using the functional variation of $\hat{p}$ in the 3-D region (see

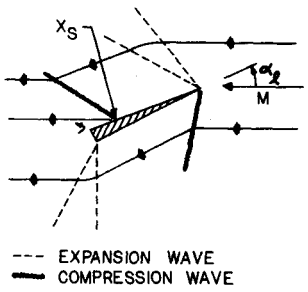

Fig. 3 Schematic of wave pattern for fin chord.

Ref. 8) and matching it to the 2-D pressure coefficient along the tip Mach cone, one obtains

$$\hat{p}_{3D} = 2\sin^{-1}\{[\beta(b_0-r)/(x-x_l)]^{1/2}\}\hat{p}_{2D}/\pi \quad \text{where} \quad r \geqq r_{3D} \tag{3}$$

For the radial coordinate of the Mach cone, r_{3D}, it can easily be shown that

$$r_{3D} = b_0-(x-x_l)/\beta \tag{4}$$

The expression for the pressure coefficient in the 3-D region, Eq. (3), assumes that the Mach cone does not intersect the body along the root chord. Therefore, it is required that $r_{3D} \geqq a$ for all freestream Mach numbers. The equation for this requirement is

$$M \geqq \{[c/(b_0-a)]^2+1\}^{1/2} \tag{5}$$

Prediction of Roll Moments

The prediction of the roll moment due to fin cant for zero angle of attack of the body and zero roll rate has been considered previously by Bolz and Nicolaides.[9] Bolz and Nicolaides derived the fin cant moment coefficient derivative, C_{l_δ}, using the linear term in the series expansion for pressure coefficient. The derivation of C_{l_δ} using the three term series expansion is given in Ref. 10 and will not be repeated here.

Consider the general case of nonzero α_b, ϕ, and δ. Using Eq. (1) and summing the differential roll moment contributed by each fin, one has

$$dl = rq\sum_{j=1}^{4}(\hat{p}_b{}^j-\hat{p}_t{}^j)\,dr\,dx$$

where the superscript j refers to the jth fin. Integrating over the surface of each fin and substituting in Eq. (3), one obtains

$$l = q\Bigg[\int_{x_l}^{x_t}\int_{a}^{r_{3D}}\sum_{j=1}^{4}(\hat{p}^j_{b_{2D}}-\hat{p}^j_{t_{2D}})r\,dr\,dx+(2/\pi)\int_{x_l}^{x_t}\int_{r_{3D}}^{b_0}\sum_{j=1}^{4}\times$$
$$(\hat{p}^j_{b_{2D}}-\hat{p}^j_{t_{2D}})\sin^{-1}\{[\beta(b_0-r)/(x-x_l)]^{1/2}\}r\,dr\,dx\Bigg] \tag{6}$$

In the analysis thus far, boundary-layer separation on the fin has not been considered. It was shown in Ref. 4 for subsonic flow that flow separation on the fin was very important for the accurate prediction of fin forces and moments at angles of attack larger than 15°. A simplified model of flow separation will be included in the present analysis by way of the pressure coefficient on the fin surface.

A schematic of the wave pattern for a cross section of the fin chord is shown in Fig. 3. Boundary-layer separation will occur on the low pressure side of the fin because of the recompression shock wave near the trailing edge. The surface pressure on the fin after the shock wave and separation will be near the freestream static pressure. As the local angle of attack increases, the shock wave strength increases and causes the separation point to move forward. At very large angles of attack the flow will separate at the leading edge and the entire surface will be in a separated flow region. The separation point will also depend on local Mach number, Reynolds number, spanwise gradient of local angle of attack, and rate of change of angle of attack if the missile is rolling. Because of lack of experimental data on almost all of these parameters, the present model of the separation point will simply depend on local angle of attack α_l. It is also assumed that after the separation point the surface pressure returns to the freestream static pressure so that the pressure coefficient is zero.

The dependence of the separation point x_s on the local angle of attack is assumed to be

$$x_s = x_l-(x_l-x_t)[1-(4\alpha_l/\pi)^2] \tag{7}$$

Two characteristics of the assumed dependence are noteworthy. First, it is postulated that the rate of change of x_s is small for small angle of attack. The accuracy of this assumption will be based in large measure on the thickness profile of the fin. For single-wedge profiles this should be a good assumption. For double-convex and double-wedge profiles, the experimental data of Ferri[11] indicate that this is not a good assumption. Second, it is assumed that leading edge separation occurs at an angle of attack of 45°. Very little experimental data is available for thin wings with sharp leading edges at very large angles of attack. From data that is available for wings at low angle of attack, however, 45° seems to be a maximum value for leading edge separation.

It can be seen from Eq. (7) that x_s is assumed to be a continuous function of α_l. However, in the real flow x_s (α_l) is probably not continuous. It is well known that the separation point is dependent on whether the boundary layer is laminar or turbulent. For high Reynolds number and low α_l, the separation should be turbulent. As α_l is increased the separation point will move forward into the transitiqnal and laminar flow. When this occurs, the separation point should jump forward because the laminar boundary layer cannot withstand an adverse pressure gradient comparable to a turbulent boundary layer. This jump would cause a discontinuity in the separation point as a function of α_l.

Returning to the roll moment equation, we now modify the pressure coefficient terms in Eq. (6) according to the foregoing discussion so that

$$\hat{p}^j = \begin{cases}\hat{p}^j & \text{for} \quad x < x_s(\alpha_l)\\ 0 & \text{for} \quad x > x_s(\alpha_l) \quad \text{and} \quad \hat{p}^j < 0\end{cases} \tag{8}$$

By this altering of the pressure coefficient it should be noted that because α_l depends on the spanwise coordinate r, separation is allowed to occur on both sides of a fin at the same time. For example, consider a fin located at the same angular position as vortex 1 and let the radial position of the vortex be less than the span of the fin. A large positive α_l would occur outboard of the vortex and separation could occur on the top surface of the fin. While at the same time, a large negative α_l would occur inboard of the vortex and separation could occur on the bottom surface of the fin.

Nondimensionalizing l with respect to $qS_b\,d$ and writing Eq. (6) in a shorter form, one finally has

$$C_l = (4/\pi d^3)\int_{x_l}^{x_t}\int_{a}^{b_0}\sum_{j=1}^{4}(\hat{p}^j_{b_{2D}}-\hat{p}^j_{t_{2D}})F(r,x)r\,dr\,dx \tag{9}$$

where

$$F(r,x) = \begin{cases}1 & \text{for} \quad r \leqq r_{3D}\\ (2/\pi)\sin^{-1}\{[\beta(b_0-r)/(x-x_l)]^{1/2}\} & \text{for} \quad r > r_{3D}\end{cases}$$

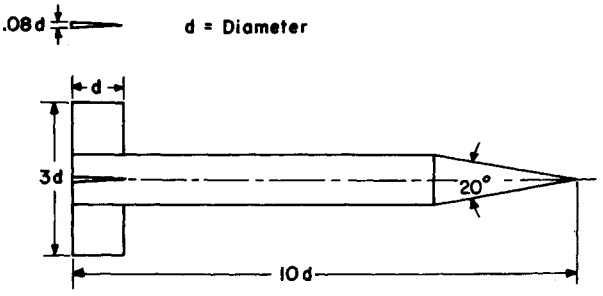

Fig. 4 Basic finner missile.

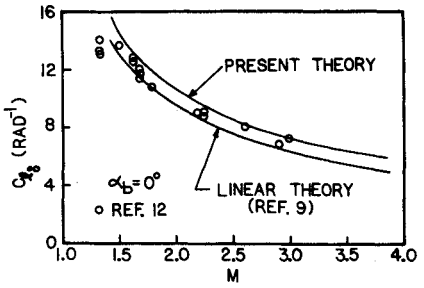

Fig. 5 C_{l_δ} vs M on the basic finner missile.

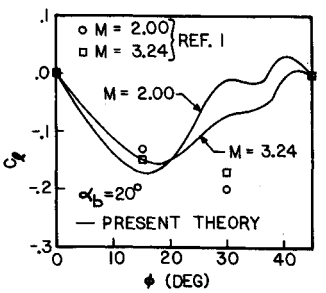

Fig. 7 Induced roll moment coefficient vs ϕ for configuration B_5W_4.

The pressure coefficients for the top and bottom surfaces of the fin depend on the turn angle of the top and bottom surfaces, $\theta_t{}^j$ and $\theta_b{}^j$, respectively. Assuming a single wedge airfoil as the basic finner missile (Fig. 4), one has

$$\theta_t{}^j = \alpha^j(r) - \theta_f \quad \text{and} \quad \theta_b{}^j = \alpha^j(r) + \theta_f$$

where

$$\alpha^j(r) = \sin^{-1}\{[\delta U_\infty \cos\alpha_b - (v_c{}^j + \dot{\phi} r \sin\phi^j)\sin\phi^j + (w_c{}^j - \dot{\phi} r\cos\phi^j)\cos\phi^j]/[U_\infty{}^2\cos^2\alpha_b + (v_c{}^j + \dot{\phi} r\sin\phi^j)^2 + (w_c{}^j - \dot{\phi} r\cos\phi^j)^2]^{1/2}\}$$

All of the numerical calculations for the present theory were performed on the University of Texas CDC 6600 digital computer. The double integration indicated in Eq. (9) was carried out by means of a 20-point Gauss-Legendre double quadrature. A typical computer run time to calculate the flowfield at the leading edge of the fin and C_l for a given missile configuration, M, δ, α_b, $\dot{\phi}$, and a set of 19 values of ϕ (e.g., $\phi = 0°$, 5°, 10°,..., 90°) takes roughly 7 sec CP time.

Discussion of Results

The fin cant moment coefficient derivative C_{l_δ} as a function of freestream Mach number for $\alpha_b = 0$ on the basic finner missile is shown in Fig. 5. It is seen that the linear theory of Boltz and Nicolaides[9] slightly underpredicts C_{l_δ} and the present theory slightly overpredicts C_{l_δ}. It should be expected that the present theory slightly overpredicts C_{l_δ} because the dynamic pressure losses due to the body boundary layer and the shock wave from the nose of the body have not been accounted for. The reason for the difference between the two theories even though $\delta \to 0$ is the fin thickness. In the linear theory, the fin thickness plays no part because $\partial\hat{p}/\partial\delta$ = constant. In the present nonlinear theory, $\partial\hat{p}/\partial\delta$ is a function of the fin thickness even though $\delta \to 0$.

The induced roll moment coefficient vs α_b for $\phi = 15°$ is shown in Fig. 6. Using the terminology given by Mello and Sivier,[1] the missile configuration is referred to as B_5W_4 (see also Ref. 10 for a description of the missile configurations). For α_b up to 20°, very good agreement between theory and experiment is obtained for $M = 3.24$; for $M = 2.0$, the theory is slightly less in magnitude than the experiment for low angles of attack. At $\alpha_b = 20°$ for $M = 2.0$ it is noted that the data exhibits a marked change in slope from negative to positive. This same characteristic has been measured in incompressible flow. Judging that the theory as presented does not exhibit this character, a numerical experiment was performed with the theory. The value of α_l which produces leading-edge separation in the theory was decreased from 45° to 22½°. The induced roll moment coefficient was then recalculated and it was found that no significant change occurred in the prediction. Therefore, a simple change in the leading-edge separation criterion does not account for the observed phenomenon.

Two possible mechanisms for the abrupt change in C_l at roughly $\alpha_b = 20°$ are suggested. First, boundary-layer separation on the fin surface may become so widespread that the flow becomes highly three dimensional. This would negate the approach of the present theory. Second, the leading edge shock may become detached. For example, the turn angle at which a plane 2-D oblique shock wave detaches at $M = 2.0$ is 23°. It is suggested that because local angles of attack can be substantially larger than α_b, shock detachment can occur when α_b is less than the 2-D shock detachment angle. When this happens, portions of the flow will become subsonic and, therefore, greatly change the pressure distribution on the fin surface.

Figure 7 shows the induced roll moment coefficient vs roll angle for $\alpha_b = 20°$ on configuration B_5W_4. It is seen that good agreement is obtained between theory and measurement at $\phi = 15°$. At $\phi = 30°$, the theory is substantially less than the two data points. More data would be very helpful in evaluating the theory for this case.

The primary reason for the rapid decrease in the magnitude of the predicted induced roll moment (Fig. 7) for $\phi > 20°$ is the vortex core region. For ϕ in this range, the positive roll moment produced by fin 1 (the fins are counted counterclockwise, starting with the fin in the range $0° \leqq \phi \leqq 90°$) is closely balanced by the negative moment produced by fin 3. The negative moment produced by fin 2 is larger in magnitude than the positive moment of fin 4 because of the clockwise velocity induced by the left body vortex. As fin 2 rotates into the vortex core, however, the induced velocity of the vortex decreases. This results in the theoretical prediction decreasing in magnitude.

The induced roll moment coefficient vs exposed semi-span $(b_0 - a)/a$ for $M = 2$ and $\phi = 15°$ is shown in Fig. 8. Excellent agreement between theory and experiment is obtained for $\alpha_b = 16°$ and fair agreement is obtained for $\alpha_b = 20°$. The present

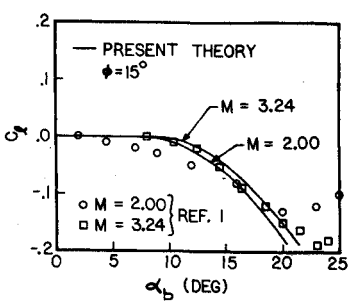

Fig. 6 Induced roll moment coefficient vs α_b for configuration B_5W_4.

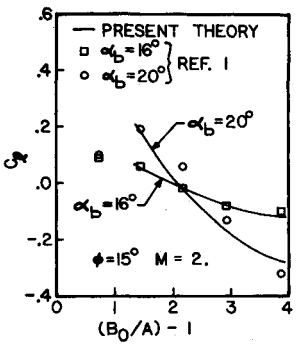

Fig. 8 Induced roll moment coefficient vs exposed semi-span.

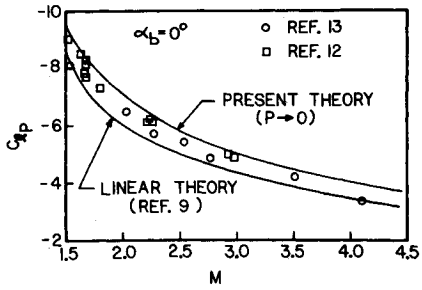

Fig. 9 C_{l_p} **vs** M **on the basic finner missile.**

theory correctly predicts the change in sign of the induced roll moment for varying span fins. As was pointed out by Mello and Sivier,[1] the spanwise location of the body vortices is of primary importance with regard to the sign and magnitude of the induced roll moment. For fin spans shorter than the radial location of the body vortices, a positive induced roll moment will be produced because of the clockwise induced velocity of the left vortex on fin 2. For a fin of somewhat larger span, the induced roll moment will be zero because the negative moment on fin 2 produced by the outboard portion will balance the positive moment of the inboard portion. As the span is made larger, the outboard portion will dominate and a large negative moment will result.

The theory is plotted in Fig. 8 down to an exposed semi-span of 1.5. Using Eq. (5) it can be calculated that this is roughly when the tip Mach cone intersects the root chord. Figure 9 shows the roll damping moment coefficient derivative C_{l_p} vs M for $\alpha_b = 0°$ on the basic finner missile. As occurred on C_{l_δ}, the present theory slightly overpredicts C_{l_p} and the linear theory slightly underpredicts C_{l_p}. The difference again between the linear theory and the present theory is the nonlinear effect of fin thickness. Roll rate, it was found, had very little effect on the roll damping moment.

Figure 10 gives C_{l_p} vs α_b for $M = 4.1$ and $p = 0.12$ for the basic finner missile. The theory predicts reasonably well the measured increase (negatively) in C_{l_p} as angle of attack increases. This follows the same trend as has been measured in incompressible flow.[4] Using the present theory it was found that the increase in C_{l_p} with α_b occurs for all supersonic Mach numbers. It was also determined from the theory that for a given α_b, C_{l_p} was almost constant with roll angle. This relationship is important if one is analyzing the dynamic roll motion of a missile in roll lock-in.

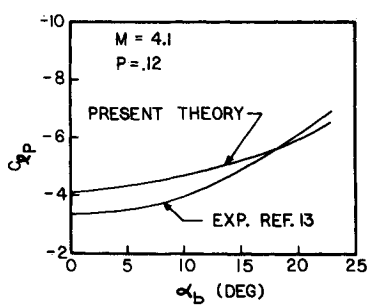

Fig. 10 C_{l_p} **vs** α_b **on the basic finner missile.**

Summary and Conclusions

A method is presented for predicting roll moments produced by finned bodies at high angle of attack in supersonic flow. Results are presented for fin cant, induced roll, and roll damping moment. The results are compared with experimental data and generally good agreement is obtained up to an angle of attack of 20°. It is shown that the theory correctly predicts the change in sign of the induced roll moment with fin span, and also the increase in roll damping moment with angle of attack.

Use of the present theory should aid the missile aerodynamicist in determining the optimum fin configuration for his requirement. Also, it should enable missile dynamicists to determine the most appropriate functional dependence of the nonlinear roll moments on angle of attack, roll angle, and roll rate.

References

[1] Mello, J. F. and Sivier, K. R., "Supersonic Induced Rolling-Moment Characteristics of Cruciform Wing Body Configuration at High Angles of Attack," *Aerospace Engineering*, Vol. 20, No. 7, July 1961, pp. 20–21, 44–51.

[2] Mello, J. F., "Investigation of Normal Force Distributions and Wake Vortex Characteristics of Bodies of Revolution at Supersonic Speeds," *Journal of the Aeronautical Sciences*, Vol. 26, No. 3, March 1959, pp. 155–168.

[3] Oberkampf, W. L. and Nicolaides, J. D., "Aerodynamics of Finned Missiles at High Angle of Attack," *AIAA Journal*, Vol. 9, No. 12, Dec. 1971, pp. 2378–2384.

[4] Oberkampf, W. L., "Aerodynamics of Finned Missiles at High Angle of Attack," Ph.D. dissertation, Department of Aerospace Engineering, Aug. 1970, University of Notre Dame, Notre Dame, Ind.

[5] Spahr, J. R., "Theoretical Prediction of the Effects of Vortex Flows on the Loading, Forces and Moments of Slender Aircraft," Tech. Rept. R-101, Jan. 1961, NASA.

[6] Jorgensen, L. H. and Perkins, E. W., "Investigation of Some Wake Vortex Characteristics of an Inclined Ogive-Cylinder Body at Mach No. 2," Rept. 1371, May 1955, NACA.

[7] Shapiro, A. H., "Oblique Shocks," *The Dynamics and Thermodynamics of Compressible Flow*, Ronald Press, New York, pp. 561–563.

[8] Bonney, E. A., "Airfoil Characteristics," *Engineering Supersonic Aerodynamics*, McGraw-Hill, New York, 1950, pp. 136–139.

[9] Bolz, R. E. and Nicolaides, J. D., "A Method of Determining Some Aerodynamic Coefficients from Supersonic Free-Flight Tests of a Rolling Missile," *Journal of the Aeronautical Sciences*, Vol. 17, No. 10, Oct. 1950, pp. 609–621.

[10] Oberkampf, W. L., "Theoretical Prediction of Roll Moments on Finned Bodies in Supersonic Flow," AIAA Paper 74-111, Washington, D.C., Jan. 1974.

[11] Ferri, A., "Supersonic Profiles," *Elements of Aerodynamics of Supersonic Flows*, Macmillan, New York, 1949, pp. 143–154.

[12] Nicolaides, J. D. and Bolz, R. E., "On the Pure Rolling Motion of Winged and/or Finned Missiles in Varying Supersonic Flight," *Journal of the Aeronautical Sciences*, Vol. 8, No. 3, March 1953, pp. 160–168.

[13] Regan, F. J., "Roll Damping Moment Measurements for the Basic Finner at Subsonic and Supersonic Speeds," Rept. 6652, March 1964, Naval Ordnance Lab., White Oak, Md.